Water Research 90 (2016) 34–43

Contents lists available at ScienceDirect

Water Research

journal homepage: www.elsevier.com/locate/watres

Biochar alleviates combined stress of ammonium and acids by firstly enriching *Methanosaeta* and then *Methanosarcina*

Fan Lü [a, b], Chenghao Luo [a], Liming Shao [b, c], Pinjing He [b, c, *]

[a] State Key Laboratory of Pollution Control and Resources Reuse, Tongji University, Shanghai 200092, China
[b] Institute of Waste Treatment and Reclamation, Tongji University, Shanghai 200092, China
[c] Centre for the Technology Research and Training on Household Waste in Small Towns & Rural Area, Ministry of Housing and Urban-Rural Development (MOHURD) of China, China

ARTICLE INFO

Article history:
Received 11 September 2015
Received in revised form
16 December 2015
Accepted 16 December 2015
Available online 19 December 2015

Keywords:
Anaerobic digestion
Ammonium toxicity
Waste treatment
Syntrophic acetate oxidation
Methanosarcinales
Interspecies electron transfer

ABSTRACT

This investigation evaluated the effectiveness of biochar of different particle sizes in alleviating ammonium (NH_4^+) inhibition (up to 7 g-N/L) during anaerobic digestion of 6 g/L glucose. Compared to the control treatment without biochar addition, treatments that included biochar particles 2–5 mm, 0.5–1 mm and 75–150 μm in size reduced the methanization lag phase by 23.9%, 23.8% and 5.9%, respectively, and increased the maximum methane production rate by 47.1%, 23.5% and 44.1%, respectively. These results confirmed that biochar accelerated the initiation of methanization during anaerobic digestion under double inhibition risk from both ammonium and acids. Furthermore, fine biochar significantly promoted the production of volatile fatty acids (VFAs). Comparative analysis on the archaeal and bacterial diversity at the early and later stages of digestion, and in the suspended, biochar loosely bound, and biochar tightly bound fractions suggested that, in suspended fractions, hydrogenotrophic *Methanobacterium* was actively resistant to ammonium. However, acetoclastic *Methanosaeta* can survive at VFAs concentrations up to 60–80 mmol-C/L by improved affinity to conductive biochar, resulting in the accelerated initiation of acetate degradation. Improved methanogenesis was followed by the colonization of the biochar tightly bound fractions by *Methanosarcina*. The selection of appropriate biochar particles sizes was important in facilitating the initial colonization of microbial cells.

1. Introduction

Ammonia (NH_3) and ammonium (NH_4^+) inhibition is a highlighted issue involved in the anaerobic digestion of organic waste and wastewater (Fotidis et al., 2013a; De Vrieze et al., 2015; Peng et al., 2015). Furthermore, ammonia inhibition has a synergetic effect with acids inhibition (Lü et al., 2013). The traditional measures of ammonia removal include pH adjustment, temperature control, biomass addition, microbial acclimation, trace elements addition, dilution and co-digestion. More recently, newer strategies to relieve ammonia inhibition have been investigated. These include removing ammonia by a side-stream (Serna-Maza et al., 2014), stripping prior to digestion (Yabu et al., 2011), biogas-recycling (Abouelenien et al., 2010), stripping assisted by water electrolysis (Park and Kim, 2015) or electrodialysis (Ippersiel et al., 2012), hollow fiber membrane contactor (Lauterböck et al., 2012; Ashrafizadeh and Khorasani, 2010), removing ammonia from recycled effluent or digestate using an additional electrochemical system (Desloover et al., 2015, 2012). Some researchers added into digester the ammonia-tolerant co-culture of syntrophic-acetate-oxidizing bacteria and hydrogenotrophic methanogens, i.e. *Clostridium ultunense* in association with *Methanoculleus* spp and *Methanoculleus bourgensis* (Fotidis et al., 2013b), or *C. ultunense*, *Syntrophaceticus schinkii* and *Tepidanaerobacter acetatoxydans* with *Methanoculleus* sp. (Westerholm et al., 2012). Researchers have also added ammonia-absorbent zeolite (Ho and Ho, 2012; Tada et al., 2005), humic acid with potential electron-accepting capability (Ho and Ho, 2012), or activated carbon (Hansen et al., 1999). Activated carbon is an absorbent, and has proven to be able to promote the direct interspecies electron transfer (DIET) between *Geobacter* and *Methanosarcinales* (Liu et al., 2012). The last four measures utilize additives that counteract ammonia toxicity and were selected according to their adsorptivity or electron transmission capacity.

* Corresponding author.
E-mail address: solidwaste@tongji.edu.cn (P. He).

http://dx.doi.org/10.1016/j.watres.2015.12.029
0043-1354/

Despite the above attempts to devise a technique to prevent ammonia toxicity during anaerobic digestion, there remains a need for simple and robust solutions that have minimal system complexity, low cost and negligible risk of second-hand pollution. Recently, researchers found that biochar promoted DIET between *Geobacter* and *Methanosarcina* (Chen et al., 2014), promoted the selective colonization of *Methanosarcina* and syntrophic bacteria (Luo et al., 2015) and had an ammonium adsorption capacity up to 17.6 mg/g (Zeng et al., 2013). Thereby, biochar has been used to reduce acid stress (Luo et al., 2015) or to improve the methanization of ethanol (Zhao et al., 2015) under anaerobic conditions. Meanwhile, porous material biochar contains certain molecular structure (e.g. average particle size of 2505 nm and a surface area 6.40 m^2/g for wood biochar obtained from 500 to 600 °C pyrolysis) (Zhang et al., 2014b). Compared with activated carbon, biochar is much affordable especially for solid waste treatment, minimizing the need for regeneration and can remain in digestates for direct use as soil amendment without separation. Therefore, eco-compatible biochar may serve as a good candidate for an additive into anaerobic digesters treating protein-rich organic solid waste, where ammonia inhibition is of great concern. Unfortunately, Mumme et al. (2014) didn't observe 3.1–6.6 g-N/L ammonium inhibition to be mitigated by pyrochar for the methane production of agricultural waste digestate. However, when the digester falls in a double risk of both acids and ammonia inhibition (Lü et al., 2013), biochar's role in counteracting ammonia has yet to be investigated.

The present investigation evaluated the effectiveness of biochar of different particle sizes to alleviate ammonium inhibition during anaerobic digestion under different ammonium "stress levels" and at the same time with acids stress. The temporal evolution and spatial allocation of microbes around biochar particles were examined closely to explain the apparent methanization performance.

2. Materials and methods

2.1. Materials

Biochar obtained from the pyrolysis of fruitwoods at 800–900 °C were ground using a mill (ZM200, Retsch, Germany), sieved to different particle sizes (i.e., 2–5 mm, 0.5–1 mm and 75–150 μm), dried at 105 °C for 24 h and then stored in a dryer for subsequent use. The water-extractable fraction of biochar had a pH of 8.63 ± 0.13 when determined by a liquid-to-solid ratio of 10:1 (v/w) using deionized water. The C and ash content of the biochar was 83.16%dw and 5.49%dw, respectively. Other characteristics of the biochar are described by Zhang et al. (2014a).

Anaerobic granular sludge was collected from a plant-scale 35 °C upflow anaerobic sludge bed reactor (Shanghai, China) with liquid internal recirculation that was treating paper mill wastewater. The collected granules of 1–3 mm was rinsed with distilled water to remove the residual wastewater, crushed under anaerobic conditions, sieved through a 1-mm mesh, and stored at −80 °C as inoculum having a total solids content of 21%wt, volatile solids content of 13%wt, and mass ratio of C:N equal to 5.25. Notable, paper mill wastewater was characterized by high concentration of chemical organic demand and very low ammonium concentration. Therefore, the inoculum used was unaccustomed to ammonium toxicity.

2.2. Experimental set-up

Batch experiments were conducted in glass serum bottles with and without 0.5–1 mm biochar at three total ammonium (TAN) "stress levels" (0.26, 3.5 and 7 g-N/L), and designated "N1" (0.26 g-N/L, without biochar), "N1CM" (0.26 g-N/L, with the medium-sized biochar), "N3" (3.5 g-N/L, without biochar), "N3CM" (3.5 g-N/L, with the medium-sized biochar), "N7" (7 g-N/L, without biochar) and "N7CM" (7 g-N/L, with the medium-sized biochar), respectively. For the 7 g-N/L stress, batch experiments with 2–5 mm and 75–150 μm biochar were also conducted to evaluate the effect of biochar particle sizes; these experiments were designated as "N7CL" (7 g-N/L, with the large-sized biochar) and "N7CS" (7 g-N/L, with the small-sized biochar). In all experiment designations "C", "L", "M" and "S" represented "biochar", "large", "medium" and "small", respectively. Further, "blank" (B) experiments were established with only 1 g-VS/L inoculum and without glucose substrate or biochar. All treatments were conducted in triplicate.

1 g-VS/L of inoculum and 10 g/L biochar was added to each batch reactor with 500 mL basic nutrient solution containing per liter 6 g glucose, 0.2 g $MgCl_2 \cdot 6H_2O$, 0.1 g $CaCl_2$, 0.2 g $Na_2S \cdot 9H_2O$, 2.77 g K_2HPO_4, 2.8 g KH_2PO_4, 0.1 g yeast extract, 5 mL trace element solution and 2 mL vitamin solution. The compositions of the trace element solution and the vitamin solution are described in Lin et al. (2013). The ratio of inoculum to substrate glucose was set at 1:6 in VS basis to introduce an acid stress status. Ammonium chloride of 1, 13.4 and 26.8 g/L was added respectively to achieve the targeted ammonium levels. The initial solution pH was adjusted to 7.0 by titration of 6 mol/L hydrochloric acid and 6 mol/L sodium hydroxide.

After being filled with the necessary reactants, the bottles were sealed with a butyl rubber and aluminum cap, sparged with N_2, incubated at 35 °C, and manually shaken every day. Gas and about 1-mL liquid samples were periodically collected under anaerobic conditions until no biogas was generated. The sampling frequencies varied according to biogas generation. Solid residues were collected at the end of the lag phase (i.e., "E", for early stage) and near the end of the methane-production phase (i.e., "F", for final, or later, stage).

2.3. Physio-chemical analysis of gas and liquids

Gas pressure in the headspace of serum bottles was determined using a manometer (Testo 512, Testo Instruments International Trading (Shanghai) Co., Ltd., Shanghai, China) to calculate the biogas production. The gas composition in terms of methane (CH_4), carbon dioxide (CO_2) and hydrogen (H_2) was analyzed using a gas chromatograph (GC9800, Shanghai Kechuang CO., LTD, Shanghai, China). Liquid samples were immediately measured for pH using a pH meter (pHS-2F, Shanghai Precision and Scientific Instrument Co., LTD, Shanghai, China) and then centrifuged at 4460 *g* for 10 min. The supernatants were analyzed for organic acids using high performance liquid chromatography (LC-20AD, Shimadzu, Kyoto, Japan), as well as for dissolved organic carbon (DOC), dissolved inorganic carbon and dissolved nitrogen (DN) using a Total Carbon/Total Nitrogen analyzer (TOC-V CPN, TNM-1, Shimadzu, Kyoto, Japan).

2.4. Methane production modeling using the modified Gompertz model

To quantitatively analyze the production of methane under various conditions, a modified Gompertz model was used as described in Lü et al. (2013) to generate three parameters: (1) the maximum CH_4 potential P (mmol-CH_4/g-glucose) at the end of incubation, (2) the maximum CH_4 production rate R_{max} (mmol CH_4/g-glucose/d) and (3) the lag phase λ (d). Each three-parameter set was estimated through global curve-fitting using Sigmaplot v12.0 (Systat Software Inc., Bangalore, India) with a minimum residual sum of squared errors between the experimental data and model curves.

To distinguish the significance of a difference between two treatments, the paired t-test was applied to the methane production curves using SPSS Statistics v17.0.

2.5. Spatial fractionation of samples for microbial analysis

The microorganisms in the liquid samples were divided into three types depending on their location in the mixture according to the protocol introduced by Luo et al. (2015): "suspended" (s), "loosely bound" (l) and "tightly bound" (t). The procedure involved repeatedly re-suspending the mixture, vortex-mixing and centrifuging it at 700 *g* in phosphate buffered saline solution containing Tween-80. In the blank treatment and treatments without biochar, only suspended microorganisms were present.

2.6. DNA extraction, "fingerprint" analysis and high-throughput sequencing of bacterial and archaeal community

The total DNA in each stratified fraction was extracted using the PowerSoil™ DNA isolation kit (Mo-Bio Laboratories Inc., CA). To characterize the bacterial and archaeal diversity and temporal evolution, automated ribosomal intergenic spacer analyses (ARISA) were conducted. The extracted DNA was amplified with primer set 1389F (5′-ACG GGC GGT GTG TGC AAG-3′) and 71R (5′-TCG GYG CCG AGC CGA GCC ATC C-3′) for archaea and with primer set ITSF (5′-GTC GTA ACA AGG TAG CCG TA-3′) and ITSReub (5′-GCC AAG GCA TCC ACC-3′) for bacteria. The polymerase chain reaction (PCR) procedure and the later data analysis was performed as previously described (Lin et al., 2013).

The DNA in fractions was further analyzed using high-throughput sequencing on an Illumina platform (Illumina Miseq PE250). The V4–V5 region of the microbial 16S ribosomal RNA gene was amplified by PCR using the primers 515F (5′-GTG CCA GCM GCC GCG GTA A-3′) and 806R (5′-GGA CTA CHV GGG TWT CTA AT-3′), which were selected as the sequencing primer set to simultaneously obtain bacterial and archaeal information (Bates et al., 2011). The pretreatment and sequencing procedure was similar to the method used by Amato et al. (2013). The raw reads were deposited into the National Center for Biotechnology Information (NCBI) Sequence Read Archive (SRA) database (Accession number: SRP043637). The individual sample reads were de-multiplexed based on the barcode tag sequence and processed as Lü et al. (2014) described.

3. Results

3.1. Methanization performance

Cumulative methane production and its Gompertz modeling parameters are shown in Fig. 1a and Table 1, respectively. Owing to the low ratio of inoculum to substrate, N1 without TAN inhibition had a long lag phase (λ) of 23.5 d and a relatively low maximum methane production rate (R_{max}) of 1.29 mmol-CH_4/g-glucose/d. As expected, higher TAN concentrations seriously prolonged λ to 30.5 d (for N3) and 63.5 d (for N7), and decreased R_{max} to 0.59 and 0.34 mmol-CH_4/g-glucose/d for N3 and N7, respectively. All biochar treatments resulted in shorter λ and higher R_{max} compared with their respective controls. Thus, N1CM reduced λ by 30.4% and increased R_{max} by 18.6% compared to N1; N3CM reduced λ by 12.7% and increased R_{max} by 10.1% compared to N3; and compared to the N7 treatment, N7CM, N7CL, N7CS reduced λ by 23.8%, 23.9%, 5.9%, respectively, and increased R_{max} by 23.5%, 47.1%, 44.1%, respectively.

The degradation of glucose followed an identical trend to methane production, as indicated by DOC concentrations (Fig. 1b). Therefore, biochar seemed to be very effective in alleviating inhibition from low pH (i.e., up to pH 4) as represented by N1 (Fig. 1c) or by severe synergetic inhibition from both acids and ammonium as represented by N7, for which a pseudo-steady-state pH of approximately 6 was set. Large-sized biochar was the most efficient in alleviating inhibition effects, followed by medium-sized particles. Although the methanization process was slower to begin with in the presence of small-sized biochar than with the larger particle sizes, the methane production rate was high once the process started.

Noticeably, as a comparison, Mumme et al. (2014) didn't observe pyrochar could mitigate strong TAN inhibition during the methane production of agricultural waste digestate. This difference might be contributed to the relatively stable substrate – digestate, the low acid level of 80 mg/L, low dosage of pyrochar addition (6.67%) in Mumme's research. Furthermore, the pyrolysis temperature and pyrolysis feedstock can alter biochar's property (Zhang et al., 2014a, 2015), which will affect biochar's function in the bioreaction.

3.2. Volatile fatty acids (VFAs) production and degradation

The concentration of volatile fatty acids (VFAs) (Fig. 2) indicates the balance between acidogenesis-acetogenesis and methanogenesis. The maximum VFAs concentrations in N3 and N7 were 66.0 and 69.0 mmol-C/L, which was lower than the concentration (87.6 mmol-C/L) in N1, suggesting that high TAN concentration had an inhibitory effect on acidogenesis. Propionate was absent in N7. For N1 and N3, biochar addition reduced the period over which acids accumulated and accelerated VFAs degradation. As to the scenarios of 7 g-N/L TAN, the addition of biochar with variant particle sizes led to the different changes of VFAs profiles. The VFAs in N7 were composed only of acetate and butyrate, and the period over which VFAs accumulated (i.e., when the concentration was higher than 50 mmol-C/L) was 60 d. In contrast, N7CL and N7CM experienced severe VFAs accumulation for only approximately 20 d, and the VFAs concentration reached a maximum of 62–71 mmol-C/L. Furthermore, the accumulated acids in N7CL and N7CM were degraded quickly. In comparison, the VFAs concentration in N7CS kept increasing over the first 60 d, reaching a maximum to 83.6 mmol-C/L, after which the concentrations sharply decreased, implying the strengthening performance of both acidogenesis and methanogenesis. Noticeably, propionate fermentation was stimulated by biochar addition, and the maximum propionate concentration increased as the biochar particle size decreased, i.e. from 18.7 mmol-C/L in N7CL, to 19.4 mmol-C/L in N7CM, and to 24.0 mmol-C/L in N7CS.

3.3. Temporal and spatial evolution of archaea

The present study investigated the microbial population not only in the later stages of anaerobic digestion, but also in the early stages, because a tremendous response in the early stages of digestion might suggest the ability of some microorganisms to acclimate to the TAN and acid stress and indicate an essential role of those "pioneers". Comparatively, the stable growth of microorganisms dominating in the later stage of digestion might only benefit from the favorable niches created by the pioneers.

The proportion of archaeal sequences in each tested sampled increased from 7.0% (±4.3%) in the early stage to 37.7% (±17.6%) in the later stage (Fig. 3), indicating the competitive growth of methanogens. *Methanobacterium* comprised the majority of the microbial population in all experiments receiving a 6 g-glucose/L organic loading. The proportion of *Methanobacterium* increased from 30.0% in the inoculum to 96.6% (N3E), 92.1% (N3CME) and 97.5% (N7E) in the early stage of digestion, and comprised 78.6% (N1F), 71.2% (N1CMF), 82.1% (N3F), 65.6% (N3CMF) and 73.6% (N7F)

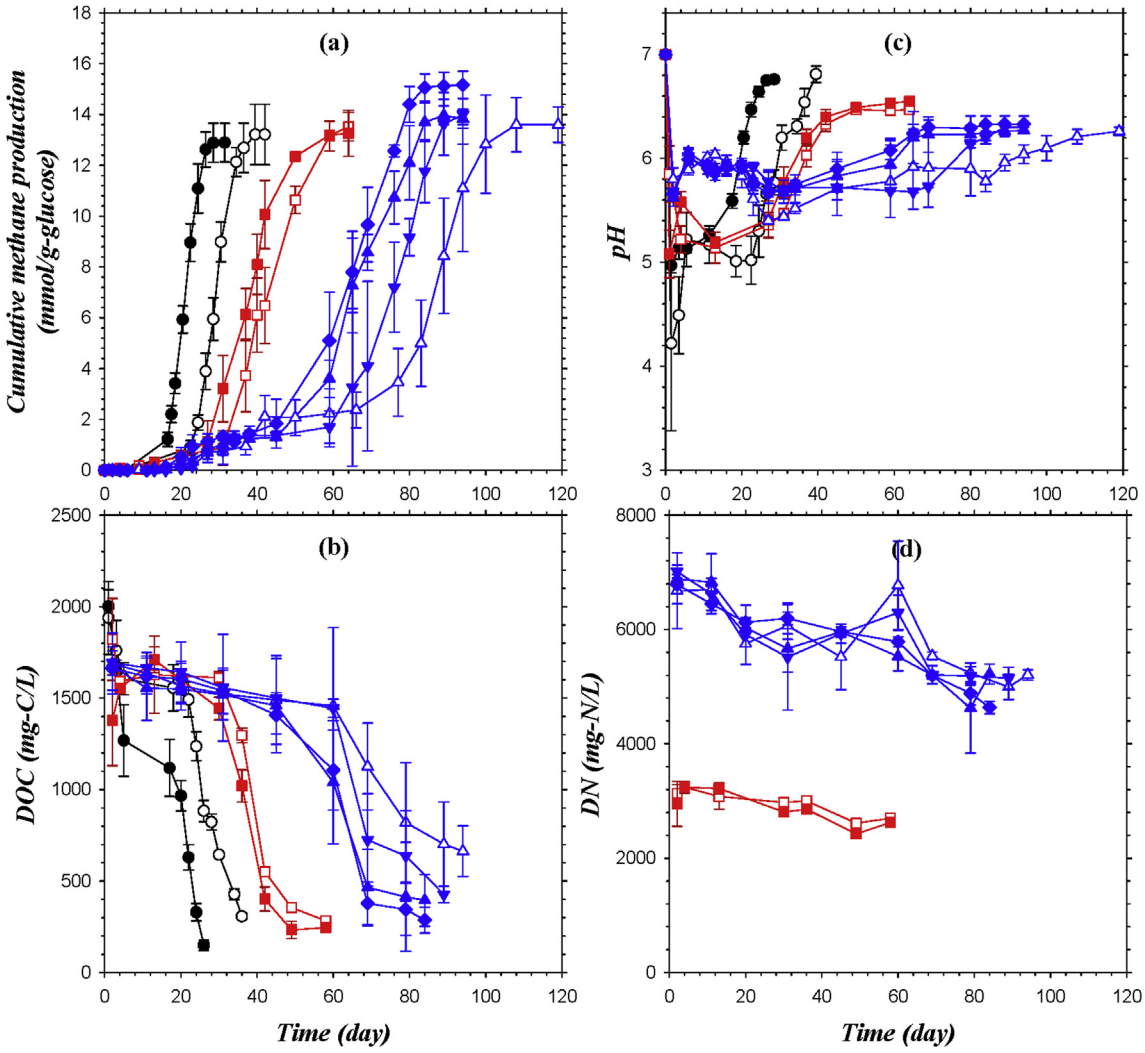

Fig. 1. Methanization performance.

Table 1
Gompertz modeling parameters describing methane production curves.

Treatment	Maximum CH_4 potential P (mmol-CH_4/g-glucose)	Maximum CH_4 production rate Rmax (mmol-CH_4/g-glucose/d)	Lag phase λ (d)	Measured final CH_4 yield (mmol-CH_4/g-glucose)
N1	13.89 ± 0.26	1.29 ± 0.07	23.46 ± 0.24	13.21 ± 1.19
N1CM	13.71 ± 0.28	1.53 ± 0.07	16.33 ± 0.18	12.89 ± 0.76
N3	14.63 ± 0.52	0.59 ± 0.04	30.46 ± 0.70	13.53 ± 0.57
N3CM	13.82 ± 0.32	0.65 ± 0.04	26.5 ± 0.64	13.26 ± 0.91
N7	16.67 ± 1.76	0.34 ± 0.04	63.51 ± 2.68	13.60 ± 0.7
N7CM	16.20 ± 1.67	0.42 ± 0.07	48.39 ± 2.86	13.83 ± 0.37
N7CL	16.67 ± 1.20	0.50 ± 0.08	48.33 ± 2.68	15.17 ± 0.53
N7CS	16.67 ± 2.34	0.49 ± 0.06	59.77 ± 1.78	14.00 ± 1.17

Note: The parameter standard errors were calculated in weighted regression. The R^2 fell in 0.979–0.998.

of the population in the later stage of digestion. *Methanosaeta* was severely suppressed (55.1% in inoculum, 2.2% in N3E and 2.5% in N7E) during the early stage of degradation of 6 g/L glucose, but slightly recovered (17.6% in N1F, 11.2% in N3F and 23.9% in N7F) in the later stage. Furthermore, the proportion of *Methanosaeta* was higher in all biochar treatments in both the early and later stages of digestion (19.5% in N1CMF; 6.4% and 15.8% in N3CME and N3CMF, respectively). Similarly, *Methanosarcina* was suppressed (8.3% in inoculum, 1.2% in N3E and zero in N7E) during the early stage of glucose degradation, and only slightly recovered in the later stage (1.9% in N1F, 6.3% in N3F and 1.2% in N7F), but was much enriched in biochar treatments (5.1% in N1CMF, 17.3% in N3CMF).

The spatial distribution of methanogens surrounding biochar particles of different sizes was closely examined in the experiments at a "stress level" of 7 g/L TAN. In the presence of large biochar particles, the proportion of archaeal sequences gradually decreased from the supernatant fraction to loosely bound and tightly bound fraction, i.e. from 16.1%, 9.4%–1.2% in early stage, and from 60.4%,

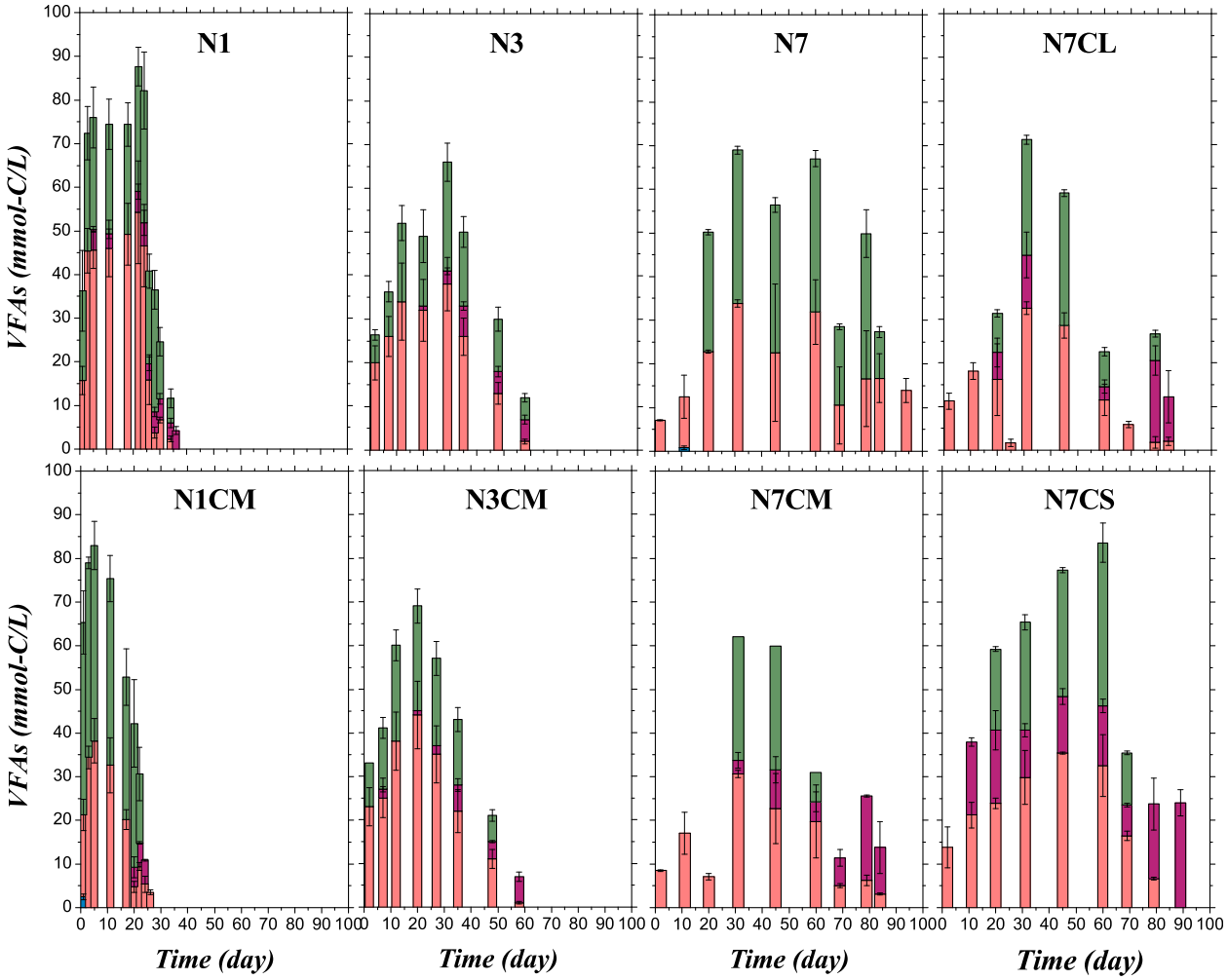

Fig. 2. Evolution of volatile fatty acids.

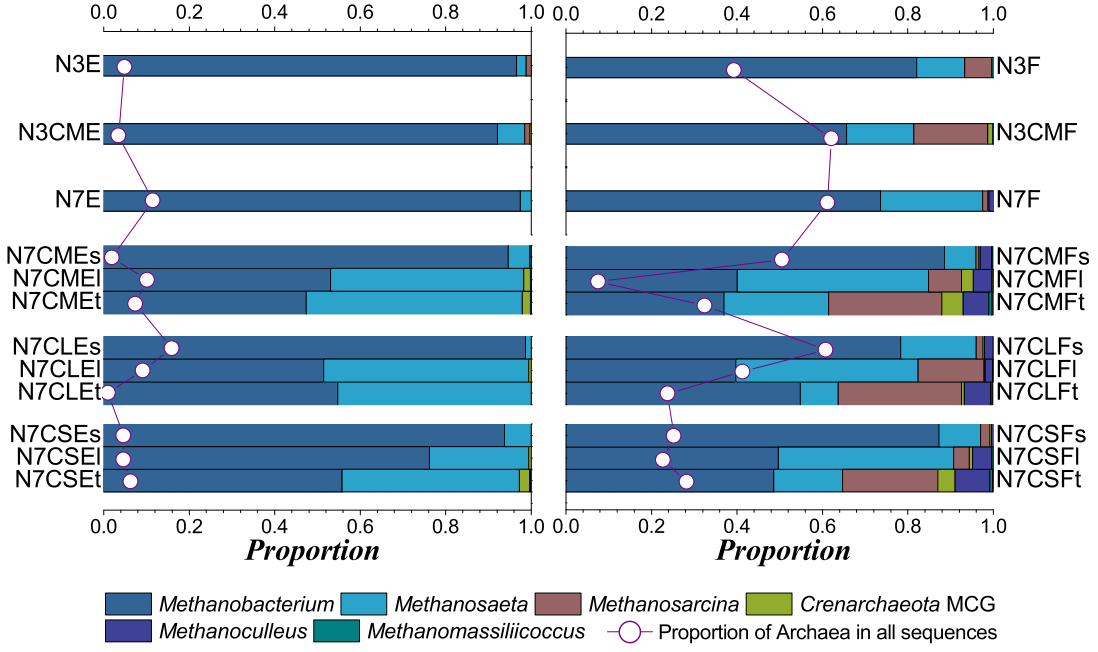

Fig. 3. Taxonomic distribution of archaea in early and later stages of digestion.

41.0%–23.7%, implying that the methanogens migrated from the outer surface to the inner sphere of the particles. *Methanosaeta* was bound almost entirely to biochar in the early stage ("s" 1.3%, "l" 47.9% and "t" 45.3%) and remained abundant in the loosely bound fraction in the later stage ("s" 17.7%, "l" 42.7%, "t" 8.9%). *Methanosarcina* was undetectable in the early stage of digestion, but gradually increased from the outer surface to the inner sphere of biochar in the later stage ("s" 1.6%, "l" 15.4% and "t" 28.8%). *Methanoculleus* followed a similar pattern, most inhabiting the tightly-bound fraction in the later stage of digestion ("s" 2.0%, "l" 1.7% and "t" 6.1%).

The spatial distribution of methanogens was almost identical on medium-sized biochar particles as on the large particles. *Methanosaeta* bound to biochar in the early stage of digestion ("s" 5.1%, "l" 45.1% and "t" 50.5%) and remained abundant in the loosely bound fraction in the later stage ("s" 7.4%, "l" 44.7% and "t" 24.4%). *Methanosarcina* ("s" 0.7%, "l" 7.7% and "t" 26.5%) and *Methanoculleus* ("s" 2.7%, "l" 4.4% and "t" 5.9%) preferred the inner sphere of biochar in the later stage of digestion. Nevertheless, the proportion of archaeal sequences was higher in biochar-bound fractions in the early stage, and was only high in supernatant and the tightly bound fraction in the later stage of digestion.

In the presence of small biochar particles, *Methanosaeta* gained dominance in the innermost layer ("s" 6.3%, "l" 23.2% and "t" 41.5%) in the early stage of digestion, and remained abundant in this loosely bound fraction in the later stage ("s" 9.7%, "l" 41.0% and "t" 16.1%). Both *Methanosarcina* ("s" 2.2%, "l" 3.7% and "t" 22.3%) and *Methanoculleus* ("s" 0.4%, "l" 4.6% and "t" 8.2%) were located mostly in the innermost parts of biochar particles in the later stage of digestion. Furthermore, the proportion of archaeal sequences was approximately the same in all three fractions, although slightly higher in the innermost, tightly bound fraction.

In brief, these data suggested that biochar prompted *Methanosaeta*, *Methanosarcina*, and the minor *Methanoculleus* to colonize the superficial layer and inner porous region of the biochar matrix.

3.4. Temporal and spatial evolution of bacteria

Bacteria were very sensitive to the incubation conditions. As a result, the bacterial profiles in both the early and later stages of digestion (Fig. 4) were totally different from that of the inoculum, which was dominated by Proteobacteria (34.3%) and Firmicutes (24.9%). The samples of early stage digestion were dominated by Enterobacteriaceae (54.6%–95.2%), which ferment glucose-derived carbon (Wust et al., 2011) and were undetected in the inoculum. The dominance of Enterobacteriaceae decreased in the supernatant (89.3%–91.1%), in the loosely bound fraction (62.9%–70.4%) and in the tightly bound fraction (54.6%–58.1%) in the 7 g-N/L TAN treatments independent of biochar particle sizes, indicating its suspended property and invasion from the outer-sphere to the inner-sphere of biochar. These changes also implied that other bacteria mainly developed from the inner pores of biochar and then expanded to the outer surface. In the later stage, the dominance of Enterobacteriaceae decreased for N1CMF (0), N3F (0.1%) and N3CMF (0.8%), but remained stable for N1F (43.0%), N7F (19.6%), N7CMF (35.9%–57.9%), N7CLF (20.3%–31.2%) and N7CSF (23.2%–61.3%), indicating the resistance of Enterobacteriaceae to TAN stress.

The dominance of other bacterial species varied with TAN concentration and with the presence or absence of biochar. The next most dominant species in the later stages of digestion was the polymer fermenter Porphyromonadaceae (48.3%) (Hahnke et al., 2015) and the glucose fermenter Christensenellaceae (13.7%) (Morotomi et al., 2012) for N3F. In N3CMF, the dominant species were Porphyromonadaceae (31.5%), a cellulose utilizer (Lü et al., 2014) and biochar favorable genus *Clostridium* (22.1%) (Luo et al., 2015). The free-living lactic acid genus *Trichococcus* (35.1%) (Pikuta and Hoover, 2014) was dominant in N7F. In N7CMF, N7CLF and N7CSF the acetogenic, sulfur-reducing (Hernandez-Eugenio et al., 2002) and potential bioelectricity generating (Chen et al., 2013; Rismani-Yazdi et al., 2013) genus *Sporanaerobacter* (8.7–2.8%) was dominant.

In the early stage of digestion, some categories of bacteria, such as the operational taxonomic unit (OTU) in Clostridiaceae, OTU in Clostridiales, urealytic *Sporosarcina* (Lauchnor et al., 2015), *Corynebacterium* and OTU in Alcaligenaceae were noticed to be associated with biochar regions. Nevertheless, owing to the difficulty in culturing these bacteria, speculating on their roles for glucose fermentation or ammonium utilization would be premature. Nonetheless, in the later stage, the syntrophic, fatty-acid-oxidizing and biofilm-producing (Cutter et al., 2003) *Syntrophomonas* was enriched in N7CMFt (8.0%) and N7CLFt (11.9%), which might suggest that biochar stimulates syntrophic bio-reactions.

3.5. Principal component analysis of microbial diversity

Fig. 5 shows the principal component analysis (PCA) of microbial diversity indicated by the high-throughput sequencing results or by ARISA identification results. In general, both for archaea and bacteria, the samples could be clustered into three groups: 1) the samples from the treatments without biochar, and from the suspended fractions, 2) the samples from the biochar-bound fractions of the early stage of digestion, and 3) the samples from the biochar-bound fractions of the later stage. Using methanogens as an example (Fig. 5a), the bi-plot clearly suggests that the suspended fractions (including those from experiments with non-biochar additives) were represented by a high proportion of hydrogenotrophic *Methanobacterium*, the biochar-bound fractions in the early stage of digestion were populated by acetoclastic *Methanosaeta*, and the biochar-bound fractions of the later stage were inhabited by archaea that could utilize multiple nutrients, i.e., *Methanosarcina* and the minors hydrogenotrophic *Methanoculleus*, *Methanomassiliicoccus* and heterotrophic Crenarchaeota group MCG. Fig. 5b shows that the abundance of the fermenter Enterobacteriaceae and Firmicutes significantly contributed to the clustering of the suspended fractions, biochar-bound fractions from the early stage of digestion, and the samples from the later stage of digestion. The PCA analysis of ARISA bands (Fig. 5c and d) supported a similar conclusion to that indicated by the PCA of sequencing results (Fig. 5a and b).

Nevertheless, the resolution of ARISA is lower than DNA sequencing, and the taxonomic assignment of ARISA bands is unknown, which makes the technique inferior to sequencing methods. However, if cost is a consideration, ARISA can be a tool for long term monitoring.

4. Discussion

The present study demonstrated that biochar was helpful in accelerating the initiation of methanization under double inhibition stress of ammonium and acids. Furthermore, the function of biochar varied with different particle sizes. Therefore, the following questions were raised and addressed.

4.1. Does biochar act through being as pH buffer or ammonium absorbent?

Since biochar is alkali (pH 8.63 ± 0.13) and porous, the first impression on biochar's function in an anaerobic process might be

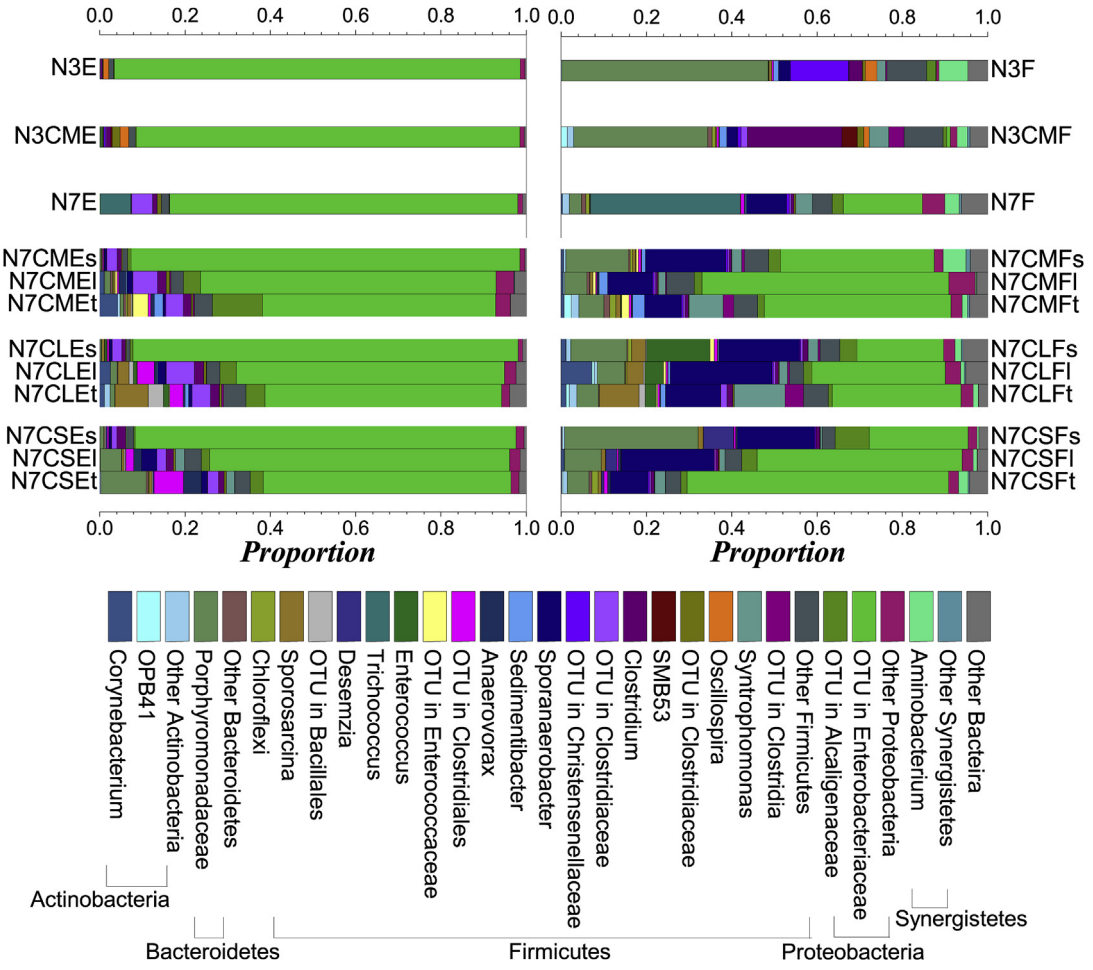

Fig. 4. Taxonomic distribution of bacteria in early and later stages of digestion.

that biochar increases pH to neutral condition or that biochar reduces ammonium concentration in the liquid fraction by surface adsorption. However, the pH on the biochar surface and its pores (microhabitat) could differ by large extent from ambient pH. Fig. 1c indicated that there was no significant difference in the ambient pH during the lag phase of the corresponding treatments with or without biochar. In the experiments that contained 7 g-N/L TAN, acidity remained at approximately pH 6, while in those containing 3.5 g-N/L TAN, pH remained at approximately 5.3. Fig. 1d indicated that there was no significant difference in the DN concentration of the corresponding treatments with or without biochar. The DN concentration decreased as incubation time increased, maybe owing to microbial utilization, since volatilization of ammonia with biogas at acidic environment could be neglected. Furthermore, we conducted an additional NH_4Cl adsorption experiment at 35 °C and an equilibrium pH 6–8; the adsorption capacity was demonstrated to be only 2–3 mg-N/g-biochar, it was in good accordance with 2.0–6.8 mg/g-pyrochar reported in Mumme et al. (2014), and was negligible for the high 7 g-N/L ammonium of the present system. Therefore, the function of biochar appeared to be biochemical, not physiochemical. The biotic promotion might be via direct interspecies electron transfer (Chen et al., 2014), through abundant functional groups on biochar surfaces (Zhang et al., 2014a, 2015), or by an enhanced surface for microbial growth. These possible functions were discussed in the following sections.

4.2. Who is the "pioneer" methanogen to initiate acetate degradation under ammonium stress?

Recent research generally is in consensus that the tandem reaction of syntrophic acetate oxidation and hydrogenotrophic methanogenesis is important for acids degradation under TAN inhibition (Fotidis et al., 2013a; Lü et al., 2013; Westerholm et al., 2012). Very recently, through stable isotopic probing, *Methanosarcina* was observed to degrade acetate by acetoclastic methanogenesis in an anaerobic digester loaded with 7 g-N/L TAN; The tolerance of this species was speculated by their aggregated form morphology (Hao et al., 2015). In the present study, the microorganisms in the samples from the early stage of digestion appeared to be a key to the initiation of methanization. As expected, hydrogenotrophic *Methanobacterium* predominated in N3E, N3CME, N7E, and in the suspended fractions of N7CE. Therefore, in the environment without biochar additives, the tandem reaction was indeed the major pathway for acids degradation. However, it was unexpected to observe the absolutely acetoclastic *Methanosaeta* thrived at a high acid concentration up to 60–80 mmol-C/L in the early stage of glucose degradation, and *Methanosaeta*'s presence was associated with biochar-bound fractions (N7CMElt, N7CLElt, N7CSElt). *Methanosaeta* has been reported to gain competitive advantage at low acid concentration (e.g., less than 1 mmol/L) (Lü et al., 2013; Karakashev et al., 2005; De Vrieze et al., 2012). However, *Methanosaeta* has a higher affinity for acetate than *Methanosarcina* (i.e., lower minimum threshold for acetate utilization)

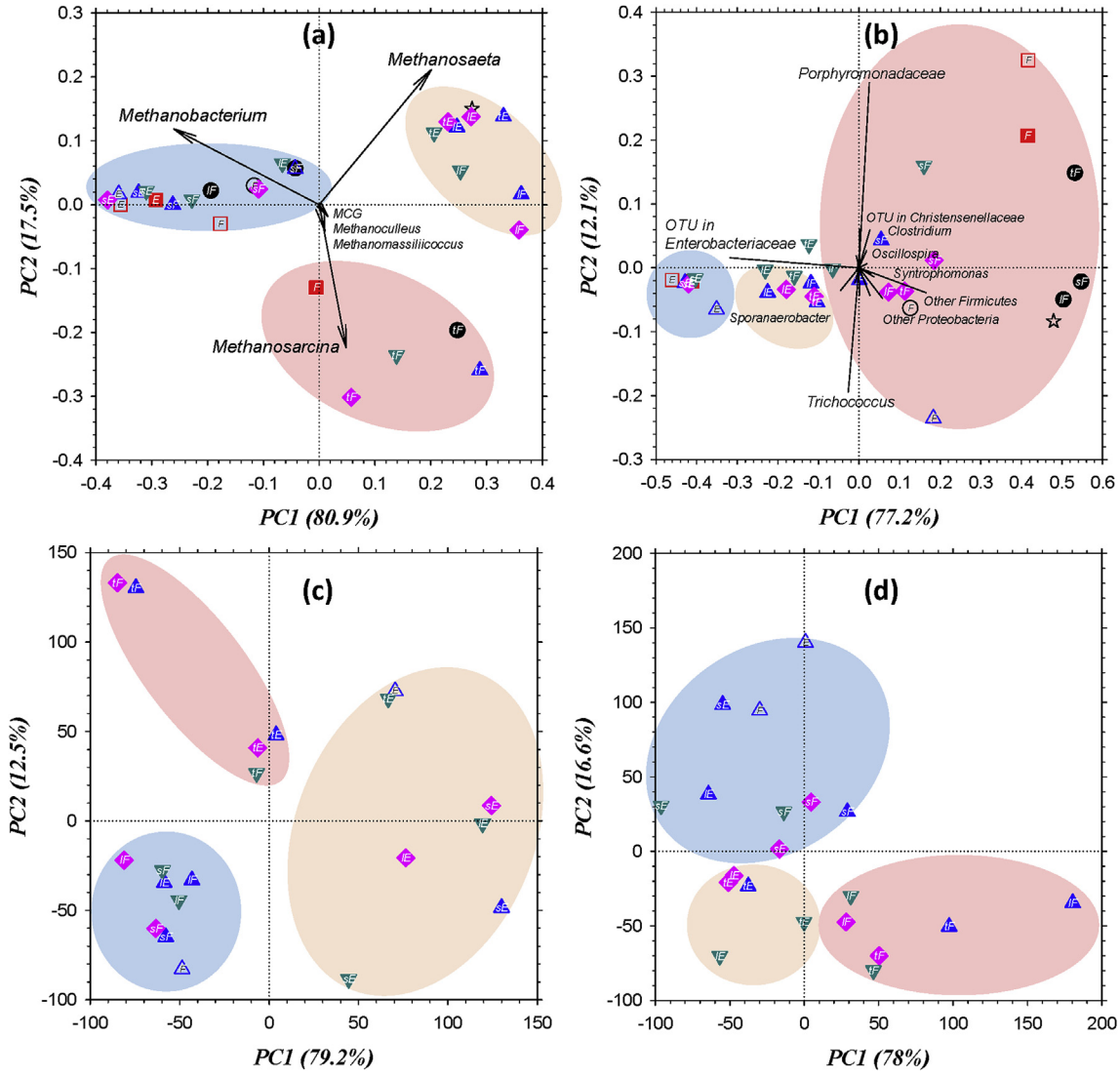

Fig. 5. Principal component analysis of microbial diversity.

(De Vrieze et al., 2012; Stams et al., 2003), and *Methanosarcina* favored the tightly-bound fractions in the later stage of digestion (Fig. 3). Thus, it appears that *Methanosaeta,* which were affinitive to biochar-associated regions, firstly utilized the acids that had diffused into biochar pores, after which the metabolically versatile *Methanosarcina*, which preferred an environment of medium TAN concentration (Lü et al., 2013), continued the acid degradation process. In the later stage of digestion, the decreased acid concentration prompted more *Methanosaeta* to stay in the loosely-bound fractions.

4.3. Does the biochar surface or the cell accessibility to internal space play a role?

Although biochar generally improved the resistance of the anaerobic digestion system to ammonium stress, the efficiency varied as a function of biochar particle size. The lag phase for methanization was reduced more by coarse- and medium-sized biochar than by fine biochar (Fig. 1); however, fine biochar promoted fermentation and acetogenesis (Fig. 2). Therefore, besides the microbial affinity to substrate, and preference for substrate, and the resistance to inhibitors, cell accessibility to the biochar surface is vital. The importance of specific surface area for methanogens seems to be negligible because fine biochar did not result in a faster initiation of methanization than did larger particles. However, the concentration of VFAs was higher in fine biochar treatments (Fig. 2), and the archaea-to-bacteria ratios were almost equal in suspended, loosely bound and tightly bound fractions (Fig. 3). Comparatively, these ratios decreased from the outer surface of particles to the inner space in coarse-particle biochar treatments, and were higher in the inner space for medium-sized biochar treatments. These observations implied that bacteria could access fine particles much easier than they could access coarse particles.

The accessibility of methanogens to biochar pores might be explained by their cell morphology. *Methanosaeta* are non-motile sheathed rods typically, 0.8–1.3 by 2–7 μm in size with long filaments (Whitman et al., 2006). *Methanosarcina* are non-motile cocci (1–2 μm) (Whitman et al., 2006) or macro-cysts up to 100 μm in diameter (Zinder et al., 1985). The width of *Methanobacterium* is 0.2–1.0 μm, while the length varies widely in the range 1.2–120 μm (Whitman et al., 2006). In terms of biochar properties, Hardie et al. (2014) found that the average median pore diameter ranged from 0.4 to 13 μm and the characteristic length of pores averaged 44 μm for acacia green waste biochar. Zhang et al. (2014b) determined

their wood biochar had an average pore size of 2.5 μm. Therefore, the biochar pore can accommodate from two to tens of methanogenic cells. The short fibrous form of *Methanosaeta* favored its movement and attachment to external pores of both coarse and fine biochar, as well as the internal pores of fine biochar. Whereas the initial colonization and possible subsequent aggregation of *Methanosarcina* could gradually block pores; such blockage would protect cells located deeper in the pores from inhibitors. Further, if *Methanobacterium* exists in the long fibrous form, the ability of the microorganism to penetrate biochar pores will be limited. Nonetheless, the above hypothesized spatial distribution needs to be proved with further direct microscopic observation.

4.4. Does direct interspecies hydrogen and/or electron transfer contribute to biochar's alleviating effect on inhibition?

According to the above discussion, the abundance of *Methanosaeta* as pioneer was enhanced by biochar addition during the initiation of methanogenesis. It then raised the question why biochar could promote its proliferation. Although porous biochar can serve as a protective environment similar to *Methanosarcina* aggregates as discussed in the section 4.3, the protection effect and the colonization amount will be significantly reduced as long as the biochar particle surface was covered by the microorganisms or contaminants. And it couldn't interpret the selective colonization of cells with comparable sizes. Therefore, methanogen's affinity to biochar needed to be explained by other long-term effects. Improved interspecies hydrogen transfer (IHT) was often accounted as the first reason to tackle ammonia inhibition (Fotidis et al., 2013b; Lü et al., 2013), where H_2 served as an electron carrier for interspecies electron transfer. In the present study, the enrichment of syntrophic acetogens *Syntrophomonas* and *Sporanaerobacter* by biochar (Fig. 4) could suggest improved IHT. However, it wasn't the dominant methanogen - hydrogenotrophic *Methanobacterium* that was promoted by biochar, implying that IHT wasn't improved by biochar. On the contrary, it was the absolutely acetoclastic *Methanosaeta* stimulated. As an alternative mechanism, DIET between *Methanosaeta* and syntrophs stood out, because *Methanosaeta* has proven to be able to directly exchange electrons with bioelectricity-generating bacteria (Rotaru et al., 2014), and the DIET function can be promoted on the surface of conductive biochar (Chen et al., 2014). Therefore, the conductive property of biochar may supplement the affinity of *Methanosaeta* to biochar surface. Compared with the vulnerable IHT link between syntrophs and hydrogenotrophic methanogens via fugitive H_2, the direct transfer of electron through a fixed conduit could facilitate the stable methanogenesis under stressed environment. Furthermore, metabolically versatile *Methanosarcina* (i.e. both acetoclastic and hydrogenotrophic) was also reported to conduct DIET (Chen et al., 2014). Combining with the evidence of *Methanosarcina*'s close association with biochar during the later stage of anaerobic digestion in the present study, it is deduced that DIET ability strenghthens the affinity of Methanosarcinales to biochar, and that Methanosarcinales counteract inhibition by improved DIET via biochar. To the last, even Methanosarcinales is far away from acetate (being both substrate and inhibitor), they can accept electron to produce methane via the conductive surface.

5. Conclusion

The addition of biochar proved to facilitate the methanization under high ammonium stress. This outcome is useful to rescue an anaerobic digester facing with the risk of ammonium or ammonia toxicity, or to enhance the process stability of a high organic loading digester treating protein-rich waste. Since biochar can be produced from several biomasses locally available, is affordable to some extent, and generally supplies a positive benefit to land ecology, it's usage and optimization in anaerobic digestion industry is highlighted. Furthermore, biochar of small particle size proved to promote the acids production, which can be further applied into the research on fermentation, acidogenesis, acetogenesis and H_2 bioproduction. Since Methanosarcinales were closely associated with biochar, the bioaugmentation of methanogens assisted by biochar or the inoculants with methanogen-rich biochar digestate also merits consideration. Meanwhile, since activated carbon has similar but strengthened properties compared to biochar, the potential function of activated carbon to release ammonia inhibition deserves re-investigation by using the similar methodology applied in the present study.

Supporting information includes Fig. S1 Evaluation of free ammonia.

Author contribution

Fan Lü designed the experimental system, worked on the microbial analysis, wrote and revised the manuscript.

Chenghao Luo worked on the incubation, measured the physiochemical parameters.

Liming Shao was involved in the result analysis and discussion of experimental data.

Pinjing He organized the research and paper preparation.

Acknowledgment

The authors would like to acknowledge the support from 973 Program (2012CB719801), NSFC (51378375, 51178327; 21177096), SHMEC Innovation Program (13ZZ030), Fundamental Research Funds for Central Universities (0400219272), the Collaborative Innovation Center for Regional Environmental Quality.

Appendix A. Supplementary data

Supplementary data related to this article can be found at http://dx.doi.org/10.1016/j.watres.2015.12.029.

References

Abouelenien, F., Fujiwara, W., Namba, Y., Kosseva, M., Nishio, N., Nakashimada, Y., 2010. Improved methane fermentation of chicken manure via ammonia removal by biogas recycle. Bioresour. Technol. 101 (16), 6368–6373.

Amato, K.R., Yeoman, C.J., Kent, A., Righini, N., Carbonero, F., Estrada, A., Rex Gaskins, H., Stumpf, R.M., Yildirim, S., Torralba, M., Gillis, M., Wilson, B.A., Nelson, K.E., White, B.A., Leigh, S.R., 2013. Habitat degradation impacts black howler monkey (Alouatta pigra) gastrointestinal microbiomes. ISME J. 7 (7), 1344–1353.

Ashrafizadeh, S.N., Khorasani, Z., 2010. Ammonia removal from aqueous solutions using hollow-fiber membrane contactors. Chem. Eng. J. 162 (1), 242–249.

Bates, S.T., Berg-Lyons, D., Caporaso, J.G., Walters, W.A., Knight, R., Fierer, N., 2011. Examining the global distribution of dominant archaeal populations in soil. ISME J. 5 (5), 908–917.

Chen, B.-Y., Hong, J., Ng, I.S., Wang, Y.-M., Liu, S.-Q., Lin, B., Ni, C., 2013. Deciphering simultaneous bioelectricity generation and reductive decolorization using mixed-culture microbial fuel cells in salty media. J. Taiwan Inst. Chem. Eng. 44 (3), 446–453.

Chen, S., Rotaru, A.-E., Shrestha, P.M., Malvankar, N.S., Liu, F., Fan, W., Nevin, K.P., Lovley, D.R., 2014. Promoting interspecies electron transfer with biochar. Sci. Rep. 4, 5019.

Cutter, L.A., Van Schie, P.M., Fletcher, M., 2003. Adhesion of anaerobic microorganisms to solid surfaces and the effect of sequential attachment on adhesion characteristics. Biofouling 19 (1), 9–18.

De Vrieze, J., Hennebel, T., Boon, N., Verstraete, W., 2012. *Methanosarcina*: the rediscovered methanogen for heavy duty biomethanation. Bioresour. Technol. 112 (0), 1–9.

De Vrieze, J., Saunders, A.M., He, Y., Fang, J., Nielsen, P.H., Verstraete, W., Boon, N., 2015. Ammonia and temperature determine potential clustering in the anaerobic digestion microbiome. Water Res. 75 (0), 312–323.

Desloover, J., Abate Woldeyohannis, A., Verstraete, W., Boon, N., Rabaey, K., 2012.

Electrochemical resource recovery from digestate to prevent ammonia toxicity during anaerobic digestion. Environ. Sci. Technol. 46 (21), 12209–12216.
Desloover, J., De Vrieze, J., Van de Vijver, M., Mortelmans, J., Rozendal, R., Rabaey, K., 2015. Electrochemical nutrient recovery enables ammonia toxicity control and biogas desulfurization in anaerobic digestion. Environ. Sci. Technol. 49 (2), 948–955.
Fotidis, I.A., Karakashev, D., Kotsopoulos, T.A., Martzopoulos, G.G., Angelidaki, I., 2013a. Effect of ammonium and acetate on methanogenic pathway and methanogenic community composition. FEMS Microbiol. Ecol. 83 (1), 38–48.
Fotidis, I.A., Karakashev, D., Angelidaki, I., 2013b. Bioaugmentation with an acetate-oxidising consortium as a tool to tackle ammonia inhibition of anaerobic digestion. Bioresour. Technol. 146 (0), 57–62.
Hahnke, S., Maus, I., Wibberg, D., Tomazetto, G., Pühler, A., Klocke, M., Schlüter, A., 2015. Complete genome sequence of the novel Porphyromonadaceae bacterium strain ING2-E5B isolated from a mesophilic lab-scale biogas reactor. J. Biotechnol. 193, 34–36.
Hansen, K.H., Angelidaki, I., Ahring, B.K., 1999. Improving thermophilic anaerobic digestion of swine manure. Water Res. 33 (8), 1805–1810.
Hao, L., Lü, F., Mazéas, L., Desmond-Le Quéméner, E., Madigou, C., Guenne, A., Shao, L., Bouchez, T., He, P., 2015. Stable isotope probing of acetate fed anaerobic batch incubations shows a partial resistance of acetoclastic methanogenesis catalyzed by *Methanosarcina* to sudden increase of ammonia level. Water Res. 69, 90–99.
Hardie, M., Clothier, B., Bound, S., Oliver, G., Close, D., 2014. Does biochar influence soil physical properties and soil water availability? Plant Soil 376 (1–2), 347–361.
Hernandez-Eugenio, G., Fardeau, M.-L., Cayol, J.-L., Patel, B.K.C., Thomas, P., Macarie, H., Garcia, J.-L., Ollivier, B., 2002. *Sporanaerobacter acetigenes* gen. nov., sp. nov., a novel acetogenic, facultatively sulfur-reducing bacterium. Int. J. Syst. Evol. Microbiol. 52 (4), 1217–1223.
Ho, L., Ho, G., 2012. Mitigating ammonia inhibition of thermophilic anaerobic treatment of digested piggery wastewater: use of pH reduction, zeolite, biomass and humic acid. Water Res. 46 (14), 4339–4350.
Ippersiel, D., Mondor, M., Lamarche, F., Tremblay, F., Dubreuil, J., Masse, L., 2012. Nitrogen potential recovery and concentration of ammonia from swine manure using electrodialysis coupled with air stripping. J. Environ. Manag. 95 (Supplement(0)), S165–S169.
Karakashev, D., Batstone, D.J., Angelidaki, I., 2005. Influence of environmental conditions on methanogenic compositions in anaerobic biogas reactors. Appl. Environ. Microbiol. 71 (1), 331–338.
Lauchnor, E.G., Topp, D.M., Parker, A.E., Gerlach, R., 2015. Whole cell kinetics of ureolysis by *Sporosarcina pasteurii*. J. Appl. Microbiol. 118 (6), 1321–1332.
Lauterböck, B., Ortner, M., Haider, R., Fuchs, W., 2012. Counteracting ammonia inhibition in anaerobic digestion by removal with a hollow fiber membrane contactor. Water Res. 46 (15), 4861–4869.
Lin, Y., Lü, F., Shao, L., He, P., 2013. Influence of bicarbonate buffer on the methanogenetic pathway during thermophilic anaerobic digestion. Bioresour. Technol. 137 (0), 245–253.
Liu, F., Rotaru, A.-E., Shrestha, P.M., Malvankar, N.S., Nevin, K.P., Lovley, D.R., 2012. Promoting direct interspecies electron transfer with activated carbon. Energy Environ. Sci. 5 (10), 8982–8989.
Lü, F., Bize, A., Guillot, A., Monnet, V., Madigou, C., Chapleur, O., Mazeas, L., He, P., Bouchez, T., 2014. Metaproteomics of cellulose methanisation under thermophilic conditions reveals a surprisingly high proteolytic activity. ISME J. 8 (1), 88–102.
Lü, F., Hao, L., Guan, D., Qi, Y., Shao, L., He, P., 2013. Synergetic stress of acids and ammonium on the shift in the methanogenic pathways during thermophilic anaerobic digestion of organics. Water Res. 47 (7), 2297–2306.
Luo, C., Lü, F., Shao, L., He, P., 2015. Application of eco-compatible biochar in anaerobic digestion to relieve acid stress and promote the selective colonization of functional microbes. Water Res. 68 (0), 710–718.
Morotomi, M., Nagai, F., Watanabe, Y., 2012. Description of *Christensenella minuta* gen. nov., sp. nov., isolated from human faeces, which forms a distinct branch in the order Clostridiales, and proposal of Christensenellaceae fam. nov. Int. J. Syst. Evol. Microbiol. 62 (1), 144–149.
Mumme, J., Srocke, F., Heeg, K., Werner, M., 2014. Use of biochars in anaerobic digestion. Bioresour. Technol. 164, 189–197.
Park, S., Kim, M., 2015. Innovative ammonia stripping with an electrolyzed water system as pretreatment of thermally hydrolyzed wasted sludge for anaerobic digestion. Water Res. 68 (0), 580–588.
Peng, W., Lü, F., Shao, L., He, P., 2015. Microbial communities in liquid and fiber fractions of food waste digestates are differentially resistant to inhibition by ammonia. Appl. Microbiol. Biotechnol. 99 (7), 3317–3326.
Pikuta, E.V., Hoover, R.B., 2014. The Genus Trichococcus. In: Lactic Acid Bacteria. John Wiley & Sons, Ltd, pp. 135–145.
Rismani-Yazdi, H., Carver, S.M., Christy, A.D., Yu, Z., Bibby, K., Peccia, J., Tuovinen, O.H., 2013. Suppression of methanogenesis in cellulose-fed microbial fuel cells in relation to performance, metabolite formation, and microbial population. Bioresour. Technol. 129, 281–288.
Rotaru, A.E., Shrestha, P.M., Liu, F., Shrestha, M., Shrestha, D., Embree, M., Zengler, K., Wardman, C., Nevin, K.P., Lovley, D.R., 2014. A new model for electron flow during anaerobic digestion: direct interspecies electron transfer to *Methanosaeta* for the reduction of carbon dioxide to methane. Energy Environ. Sci. 7 (1), 408–415.
Serna-Maza, A., Heaven, S., Banks, C.J., 2014. Ammonia removal in food waste anaerobic digestion using a side-stream stripping process. Bioresour. Technol. 152 (0), 307–315.
Stams, A.J.M., Elferink, S.J.W.H.O., Westermann, P., 2003. Metabolic interactions between methanogenic consortia and anaerobic respiring bacteria. In: Ahring, B., Angelidaki, I., de Macario, E.C., Gavala, H.N., Hofman-Bang, J., Macario, A.J.L., Elferink, S.J.W.H.O., Raskin, L., Stams, A.J.M., Westermann, P., Zheng, D. (Eds.), Biomethanation I. Springer, Berlin Heidelberg, pp. 31–56.
Tada, C., Yang, Y., Hanaoka, T., Sonoda, A., Ooi, K., Sawayama, S., 2005. Effect of natural zeolite on methane production for anaerobic digestion of ammonium rich organic sludge. Bioresour. Technol. 96 (4), 459–464.
Westerholm, M., Levén, L., Schnürer, A., 2012. Bioaugmentation of syntrophic acetate-oxidising culture in biogas reactors exposed to increasing levels of ammonia. Appl. Environ. Microbiol. 78 (21), 7619–7625.
Whitman, W., Bowen, T., Boone, D., 2006. The methanogenic bacteria. In: Dworkin, M., Falkow, S., Rosenberg, E., Schleifer, K.-H., Stackebrandt, E. (Eds.), The Prokaryotes. Springer, New York, pp. 165–207.
Wust, P.K., Horn, M.A., Drake, H.L., 2011. Clostridiaceae and Enterobacteriaceae as active fermenters in earthworm gut content. ISME J. 5 (1), 92–106.
Yabu, H., Sakai, C., Fujiwara, T., Nishio, N., Nakashimada, Y., 2011. Thermophilic two-stage dry anaerobic digestion of model garbage with ammonia stripping. J. Biosci. Bioeng. 111 (3), 312–319.
Zeng, Z., Zhang, S.D., Li, T.Q., Zhao, F.L., He, Z.L., Zhao, H.P., Yang, X.E., Wang, H.L., Zhao, J., Rafiq, M.T., 2013. Sorption of ammonium and phosphate from aqueous solution by biochar derived from phytoremediation plants. J. Zhejiang Univ. Sci. B 14 (12), 1152–1161.
Zhang, J., Lü, F., Luo, C., Shao, L., He, P., 2014a. Humification characterization of biochar and its potential as a composting amendment. J. Environ. Sci. 26 (2), 390–397.
Zhang, J., Lü, F., Shao, L., He, P., 2014b. The use of biochar-amended composting to improve the humification and degradation of sewage sludge. Bioresour. Technol. 168, 252–258.
Zhang, J., Lü, F., Zhang, H., Shao, L., Chen, D., He, P., 2015. Multiscale visualization of the structural and characteristic changes of sewage sludge biochar oriented towards potential agronomic and environmental implication. Sci. Rep. 5, 9406.
Zhao, Z., Zhang, Y., Woodard, T.L., Nevin, K.P., Lovley, D.R., 2015. Enhancing syntrophic metabolism in up-flow anaerobic sludge blanket reactors with conductive carbon materials. Bioresour. Technol. 191 (0), 140–145.
Zinder, S.H., Sowers, K.R., Ferry, J.G., 1985. *Methanosarcina thermophila* sp. nov., a thermophilic, acetotrophic, methane-producing bacterium. Int. J. Syst. Evol. Microbiol. 35 (4), 522–523.